



Royal Military Academy
Polytechnic Faculty
CISS Department

Neural-network based sea/ice discrimination using ERS scatterometer data.

Khaoula Hmamouche

August 2015

The work has been performed at the Royal Military Academy of Belgium, funded by an educational grant in the frame of the ESA Contract "Setup of the Scatterometer Instrument Competence Centre – SCIRoCCo"

Intern-ship report
Neural-network based sea/ice discrimination using ERS
scatterometer data.

Khaoula Hmamouche

Department of Communication, Information, Systems and Sensors
Royal Military Academy, 30 av de la Renaissance, B-1000 Brussels, Belgium
17 August 2015

Supervisors: Prof. Xavier Neyt
Anis Elyouncha

Contents

1. Introduction	3
2. Ice detection algorithm overview	4
3. Improvement of the ice detection	5
4. Kp parameter, Standard Deviation	5
5. Backscatter noise	7
6. Performance comparison of the individual criterion	7
7. Results	9
8. Conclusions	10
9. References	10

1. Introduction

The ERS-2 scatterometer is a radar working at 5,3 GHz. The measurements produced by this radar allow retrieving of important geophysical parameters as: the wind fields over oceans, the sea-ice coverage, the soil moisture...etc.

This radar has three antennas looking 45° forward, backward and sideways, called fore, mid and aft antenna respectively. Measurements taken from three directions allow the determination of the wind direction.

The radar antennas illuminates a swath of approximately 500 km width is parallel to the sub-satellite track. A regular grid of nodes, separated by 25 km, is defined inside the swath, and the final measurements are given at each of these nodes.

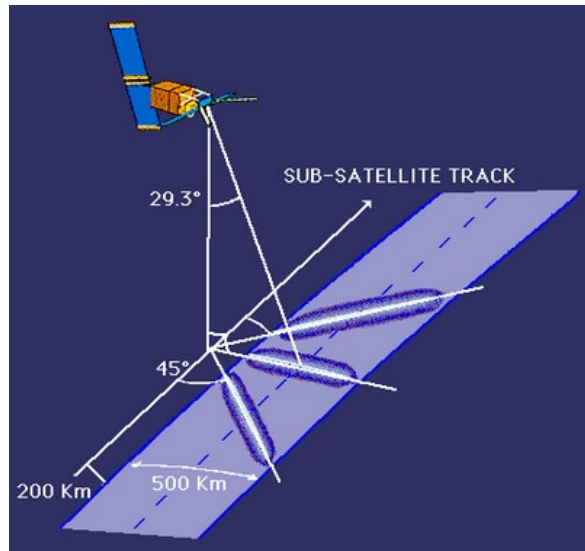


Figure1: The ERS Satellite scatterometer

The primary objective of the scatterometer is to determine the wind fields over oceans using empirical Geophysical Model Functions (GMF). These models are only valid over open sea, they are not valid over land and sea-ice. Land is easily discarded using land masks. Over sea-ice it is more difficult to discriminate open water and the ice due to the dynamic extent of the sea-ice which result from the freezing and melting through the seasons. So as to remove spurious wind vectors we have to discriminate the sea and the ice at real time.

A neural-network has been developed (Ref. 5, Ref. 6), to compute the sea/ice probability $P(H1|m_c)$ at each node of the grid. (where: $H1$ is the hypothesis the measurement corresponds to ice, given the measurement vector $m_c = (C_c; n)$, n is the node number in which the measurement C_c was made).

Some criteria can be used such as: derivative of sigma, backscatter isotropy, distance to the wind model and distance to ice model. This work is an attempt to enhance the sea-ice detection algorithm by adding other criteria while the stateless strategy will be the same.

The K_p parameter, the standard deviation and the noise power may be sensitive to the difference between ocean and sea-ice and will be considered.

2. Ice detection algorithm overview

Given the measurement, the goal is to compute the probability $P(H1|m_c)$. A Multi-Layer Perceptron (MLP) of one hidden layer containing 5 neurons is used. This MLP has two inputs: one for the criterion itself and one for the node number. If the criterion is a vector of two elements $(C_{c(1)}, C_{c(2)})$, which means 3 inputs, the MLP needs to have two hidden layers containing 10 neurons each. (*Ref. 5, Ref.6*)

The neural-network is trained using the IFREMER sea-ice map as reference, it provides the ice probability as output. In order to perform a classification, this probability is thresholded.

The various criteria which were used to discriminate the sea-ice and the open water are:

The distance to ice model:

The idea is to use the euclidean distance to ice model as discriminating criterion. The model used is the ERS ice model, which is described in *Ref. 4*. It consists in an incidence angle-dependent line in the $(\sigma_f, \sigma_a, \sigma_m)$ space.

The distance to wind model:

The GMF allows retrieving wind speed and direction from measured backscatter. The euclidean distance to the wind model was, hence, proposed as a discriminating criterion in *Ref. 1*. The backscatter measurements acquired over sea-ice should lie close to the wind model, while measurements performed over ice might be located further away from the wind model. However, since the σ_o measurements over ice are actually very close to the wind model at mid swath, this criterion will not be very discriminating at mid swath. We are going to use the enhanced distance to wind model criterion (the fusion of the distance to ice model and the direction of the wind using the symmetric associative sum operator, *Ref. 6*), because it is much more discriminant than the original criterion.

The derivative of the backscatter in function of the incidence angle:

In *Ref. 3*, the derivative of the backscatter was proposed as discriminating criterion. Generally, the sigma derivative (slope) over the sea is larger than over sea-ice. The derivative of the backscatter can be written as:

$$D = -\frac{(\sigma_f + \sigma_a)/2 - \sigma_m}{(\theta_f + \theta_a)/2 - \theta_m}$$

Where σ_f , σ_a and σ_m are the fore, aft and mid-beam measurements of the backscatter made at different angles (in dB), and Θ_f , Θ_a and Θ_m are the incidence angles for the fore, aft and mid antennas (in degree).

The backscatter anisotropy:

In *Ref. 2*, the backscatter anisotropy factor is proposed as discriminating criterion, it is defined as:

$$A = \left| \frac{\sigma_f - \sigma_a}{\sigma_f + \sigma_a} \right|$$

Where σ_f and σ_a are the fore and aft-beam measurements of the backscatter provided in dB. Ice has a low isotropy factor because it is supposed to be isotropic as EM backscattering is concerned. Furthermore, the open sea generally results in a high isotropy factor, because of the wind. However, low isotropy values can be measured over the sea. This occurs when the wind is blowing parallel or perpendicular to the satellite ground track.

Figure 2,3,4 and 5 show the output of the neural network $P(HI|m_c)$, respectively, for the distance to ice model, the distance to wind model, the derivative of sigma and the sigma anisotropy.

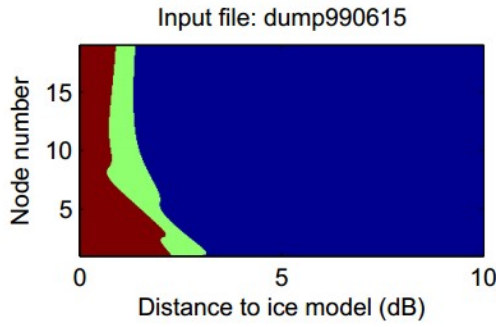


figure 2: Thresholded probability $P(HI|m_c)$ for the distance to ice model
Number of sea nodes: 15244

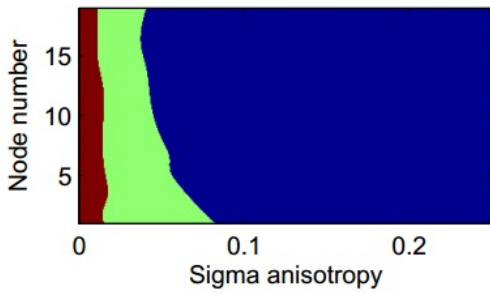


figure 4: Thresholded probability $P(HI|m_c)$ for the derivative of sigma

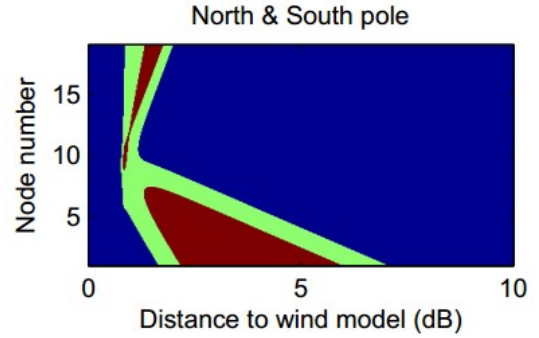


figure 3: Thresholded probability $P(HI|m_c)$ for the distance to wind model
Number of ice nodes: 27088

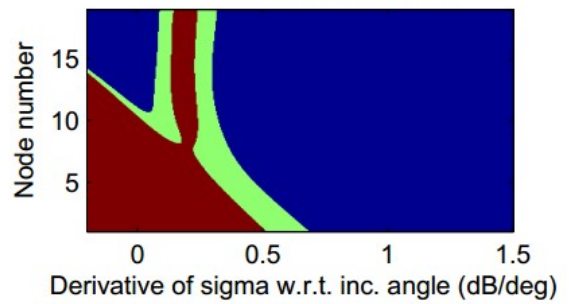


figure 5: Thresholded probability $P(HI|m_c)$ for the sigma anisotropy

The Blue colour corresponds to $P < 20\%$ (Ocean with 80% probability).
The red colour corresponds to $P > 80\%$ (Ice with 80% probability)
And the green colour corresponds to the intermediate probabilities.

Based on figures above and comparing the various criteria, we conclude that the two best criteria are: the distance to ice model and the derivative of sigma. The area of uncertainty (the green area), corresponding to ice probabilities: $20\% < P < 80\%$ is small for these two criteria.

3. Improvement of the ice detection

In an attempt to enhance the ice detection algorithm, we introduce new criteria which can be combined with the other discriminating criterion seen in the previous paragraph (Ice detection algorithm overview).

In this paper, the standard deviation and the noise power are added as criteria to discriminate the ice and the open water, and combined with the other criteria specially the best sources of information as the distance to ice model, the derivative of sigma and the distance to the wind model taking into account the relative wind direction, using the existing combination methods (Ref. 9).

4. Kp parameter, Standard Deviation

The Kp parameter and the standard deviation are complementary data relative to the accuracy of the σ_o values which are determined for each node and each beam. The Kp parameter is related to the noise-to-signal ratio with the following formula:

$$Kp = (1 + \overline{\sigma_{o,noise}} / \overline{\sigma_o}) / M$$

where M is the effective number of independent signal samples, $\overline{\sigma_o}$ is the average of the measurements of σ_o and $\overline{\sigma_{o,noise}}$ is the $\overline{\sigma_o}$ equivalent of the noise power.

In practice the Kp parameter is computed as the normalized standard deviation according to the following formula:

$$Kp = 100 \frac{SD(\sigma_0)}{\bar{\sigma}_0}$$

The Kp parameter is reported in the scatterometer products for each beam and node. The standard deviation is deduced from the Kp parameter and the backscatter σ_0 according to the following formula:

$$SD(\sigma_0) = Kp \bar{\sigma}_0$$

In order to assess the sensitivity of the standard deviation and based on the IFREMER data, acquired during January 1999, the graphs below are produced. These graphs show the spatial distribution of the standard deviation over the South and the North Pole.

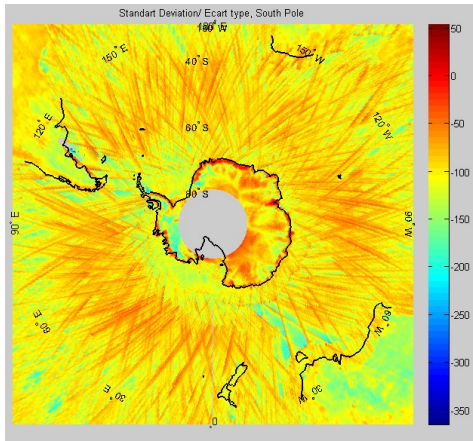


Figure 7: Standard deviation Map (South Pole)

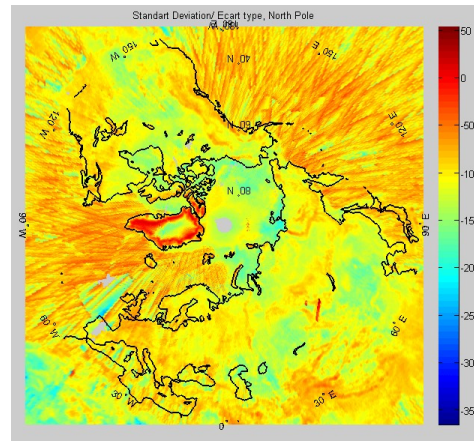


Figure 8: Standard deviation Map (North Pole)

From figures 7 and 8, we notice that the standard deviation takes, in average, different values over ice and over open water. We notice that the values of the standard deviation over the ice are lower than its values over open water. Nevertheless, the values of the standard deviation are also small over some homogeneous land areas such as forests and deserts.

Figures 9 and 10 show the distribution of the Kp parameter and the standard deviation for the sea and the ice classes as a function of the incidence angle.

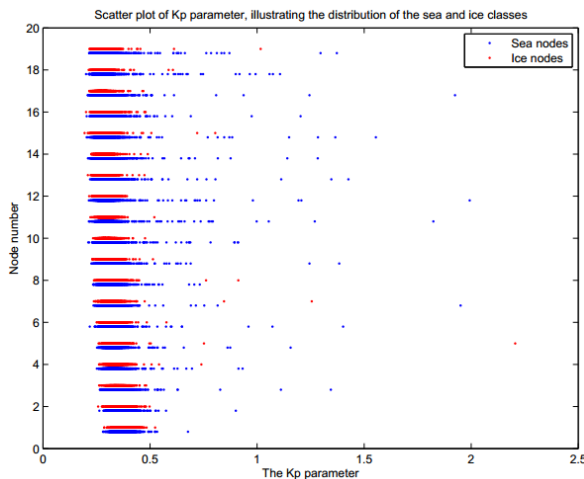


Figure 9: Distribution of the Kp parameter for the sea and ice classes.

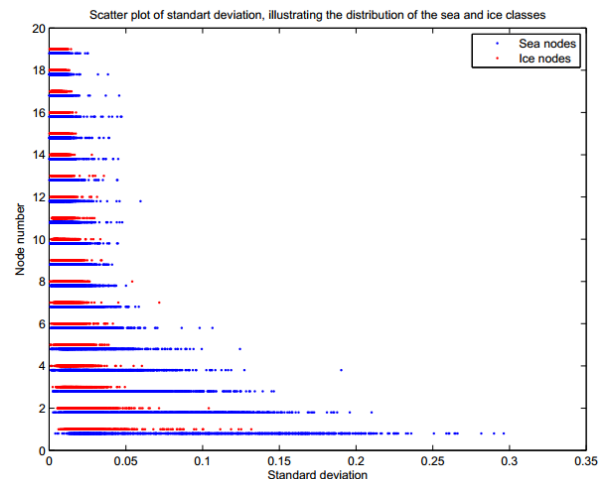


Figure 10: Distribution of the standard deviation for the sea and ice classes.

As we can see in the figures above, the measurements of the Kp parameter does not allow the sea/ice discrimination. The standard deviation is more discriminant than the Kp parameter, especially at low incidence angles. The values of the standard deviation over the sea are greater than its values over the ice.

5. Backscatter noise

The scatterometer measures the backscattering coefficient of distributed targets with additive noise to the received signal. Consequently, the noise power has to be measured separately in order to determine the signal-only power, according to the following formula (Ref. 8):

$$P_s = P_{s+n} - P_n$$

where P_{s+n} is the signal + noise power, P_n is the noise power and P_s is the signal-only power.

The noise signal is composed of the receiver thermal noise, which represent the instrument noise: P_{nr} , and the earth's thermal radiation integrated over the viewed ground: P_{na} . This second component has to be exploited as it changes spatially, temporally and with the viewing geometry and can be combined with the distance to ice model and the derivative of sigma. However, the thermal radiation is constant over the antenna footprint. Figures 11 and 12 show the noise map in the north and south pole respectively.

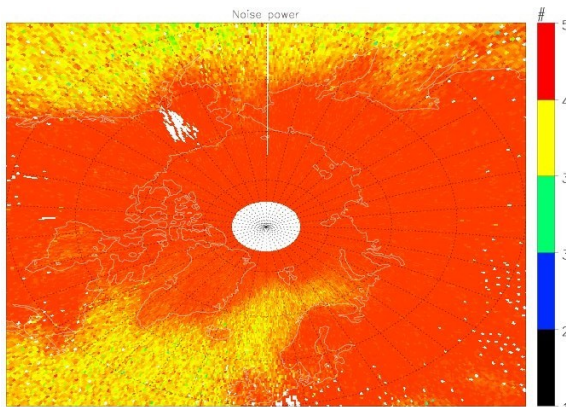


Figure11: Noise Map (North Pole)

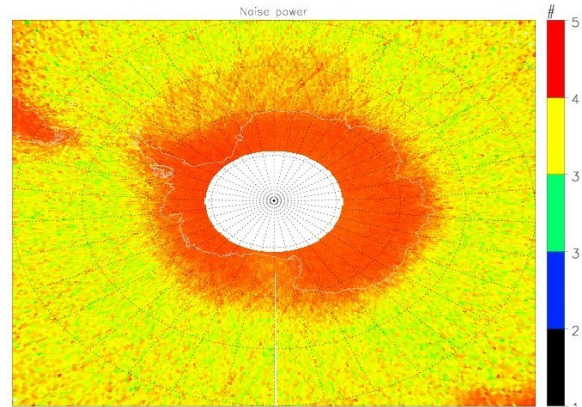


Figure12: Noise Map (South Pole)

As can be seen from figures above, the noise takes higher values over land and over the ice, moreover the measurements over the boundaries which separate the ice and the sea are not accurate due to the very low spatial resolution of the noise signal. Noise-data provided by the scatterometer corresponds to the whole swath. Consequently the noise is not a very discriminant criterion.

6. Performance comparison of the individual criteria

The outputs of to the neural-network after training corresponding to the Kp parameter and the standard deviation, are represented, respectively, in figures 13 and 14.

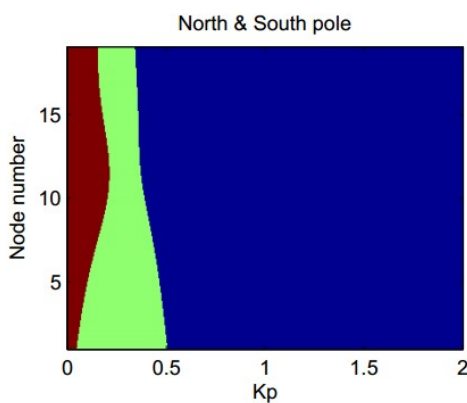


Figure 13: Kp parameter

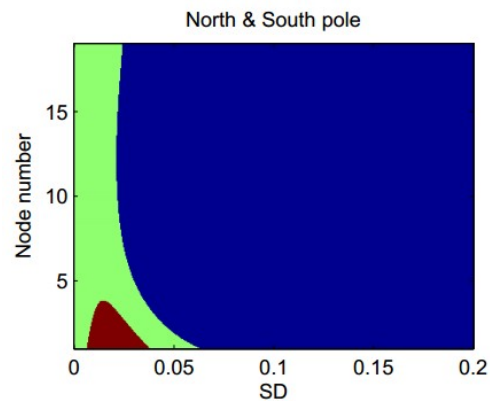


Figure 14: Standard Deviation

As can be seen from figures 13 and 14 the area of uncertainty corresponding to ice probabilities: $20\% < P < 80\%$ are large for both Kp parameter and the standard deviation.

The Receiver-Operating Characteristic (ROC) is used to assess the classifier performance. The ROC is a plot of the true ice rate against false ice rate for varying threshold considered. A plot of the unclassified rate is also used to compare the different criteria and their combination

The unclassified rate as a function of the node number is shown in figure 15, and the ROC (Receiver-Operating Characteristic) for ice for the different criteria is shown in the figure 16.

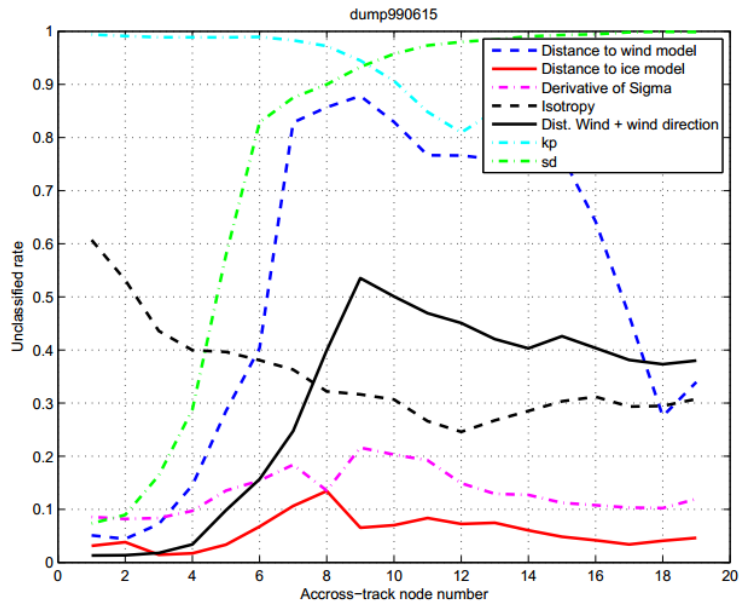


Figure15: The unclassified rate for the different criteria in function of the node number for a false classification of 3%.

We notice that the standard deviation is more discriminant than the Kp parameter.

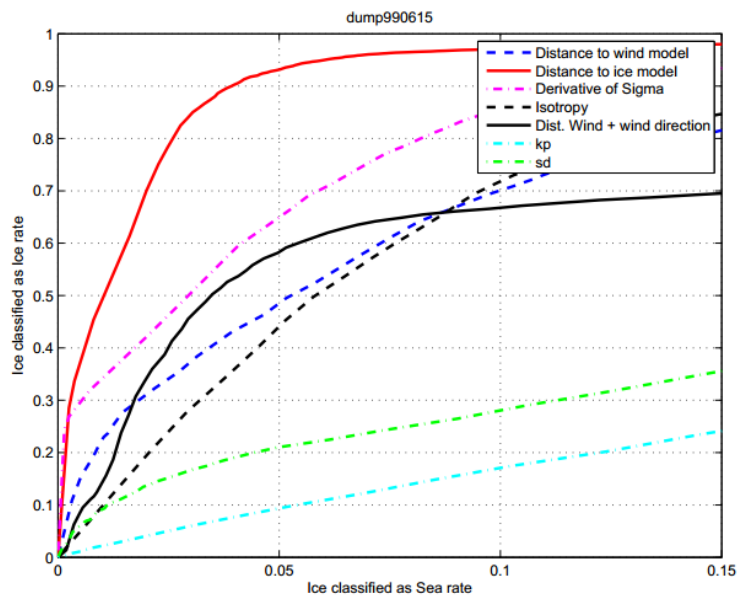


Figure 16: The Receiver-operating characteristic comparing the different discriminating criteria

As can be seen from figures 15 and 16, the Kp parameter and the standard deviation have a poor performance compared to the other criteria.

7. Results

The fusion of the different criteria is used to reduce the imprecision and the uncertainty. To compute the fusion of the neural-network outputs, the operator used is the mean operator, which relate the ice probability, P_1 and P_2 , of two different criteria by to the following expression:

$$m(P_1, P_2) = (P_1 + P_2) / 2$$

This formula can be readily extended for any number of measurements. We could also use the symmetric associative sum operator, (Ref. 5, Ref. 6) which equation is written as:

$$s(P_1, P_2) = (P_1 P_2) / (P_1 P_2 + (1 - P_1)(1 - P_2))$$

However this operator performs slightly worse than the mean operator, which could be due to the fact that the criteria combined are not totally independent.

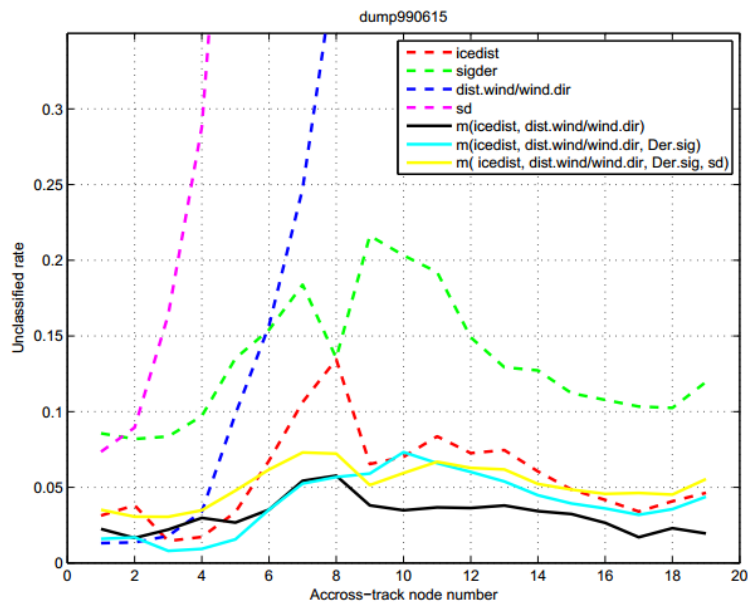


figure 17: Unclassified rate for different fusions of the criteria

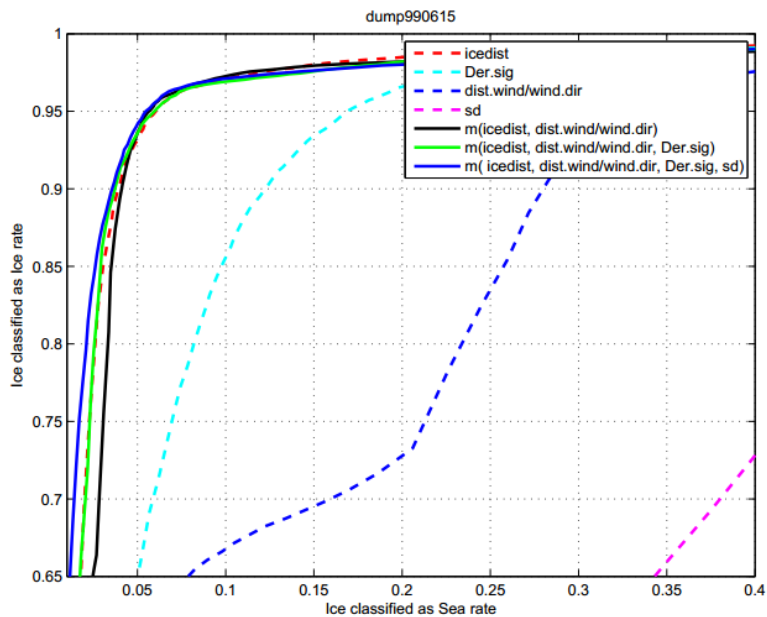


figure 18: Receiver-operating characteristic comparing different fusions of the criteria

In all figures above:

icedist denotes: *the distance to ice model.*

dist.Wind/ wind.dir denotes: *the distance to wind model and the wind directions (Ref. 6).*

sd denotes: *the standard deviation.*

Kp denotes: *the Kp parameter.*

Der.sig denotes: *the derivative of sigma.*

M denotes: *the mean operator.*

The standard deviation, $SD(\sigma_o)$, performs worse than the other criteria, however its fusion with the Distance to ice model and the derivative of sigma enhances the performance, as the blue curve shows, but only for low false positive rate.

The sea/ice discrimination criteria: standard deviation and the noise do not enhance the algorithm as foreseen.

8. Conclusions

Using a neural-network framework and the ERS scatterometer data, we reviewed the standard deviation and the noise as sea/ice discrimination criteria and compared them to the existing criteria. We used the neural-network framework because it consists on thresholding the conditional ice probability with clear trade offs.

The results of the comparison show clearly that the standard deviation and the noise perform worse than all the other existing criteria. The accuracy and the decisiveness of the results obtained by the fusion of an individual criterion are enhanced. Indeed, despite the poor performance of the standard deviation, its fusion with the distance to ice model, the derivative of sigma and the distance to wind model improves the precision of the result.

These results are more accurate than what we got before (Ref. 6), especially in the region of the curve with low false positive rate (Ice classified as sea rate). Therefore, the standard deviation does not improve the results as expected.

9. References

1. Gohin, F. and Maroni, C. "ERS scatterometer polar sea ice grids: User manual". *Technical Report C2-MUT-W-03-IF, IFREMER, March 1998*
2. A. Cavanié, F. Gohin, Y. Quilfen, and P. Lecomte, "Identification of sea ice zones using the AMI-wind: Physical bases and applications to the FDP and CERSAT processing chains", in *Proc. Second ERS-1 Validation Workshop, pp.1009-1012, ESTEC (Hamburg, Germany), Oct.1993.*
3. Gohin, F. and Cavanié, A. "Some active and passive microwave signatures of antarctic sea ice from mid-winter to spring 1991". *International Journal of Remote Sensing, 16(11), pp. 2031-2054, 1995.*
4. S. de Haan, S. and A. Stoffelen, "Ice discrimination using ERS scatterometer". *Technical report, KNMI, September 2001*
5. Xavier Neyt, Pauline Pettiaux, Nicolas Manise and Marc Achery. "Neural-network based stateless ice detection in ERS scatterometer data". *In Proceedings of the Envisat Symposium, Salzburg, Austria, September 2004.*
6. Xavier Neyt, Nicolas Manise and Marc Achery. "Enhanced neural-network based sea/ice discrimination using ERS scatterometer data". *Proc. SPIE 5977, Remote Sensing of the Ocean, Sea Ice, and Large Water Regions, (October 18, 2005).*
7. Pascal Lecomte "The ERS Scatterometer instrument and the On-Ground processing of its Data". *in Proceedings of a Joint ESA-Eumetsat Workshop on Emerging Scatterometer Applications – From Research to Operations, pp. 241–260, ESTEC, (The Netherlands), Nov. 1998*
8. Anis Elyouncha "Analysis of C-band spaceborne scatterometer thermal noise". *In Proc. SPIE 9240, Remote Sensing of the Ocean, Sea Ice, Coastal Waters, and Large Water Regions, Amsterdam, 2014.*
9. I.Bloch, "Information combination operators for data fusion: A comparative review with classification", *IEEE Transactions on Systems, Man and Cybernetics 26, pp.52-67, Jan. 1996.*